Research in Veterinary Science 105 (2016) 92–102

Contents lists available at ScienceDirect

Research in Veterinary Science

journal homepage: www.elsevier.com/locate/rvsc

M1 and M2 macrophage recruitment during tendon regeneration induced by amniotic epithelial cell allotransplantation in ovine

Annunziata Mauro [a,b], Valentina Russo [a,b,*], Lisa Di Marcantonio [a], Paolo Berardinelli [a], Alessandra Martelli [a], Aurelio Muttini [a,b], Mauro Mattioli [a], Barbara Barboni [a,b]

[a] Faculty of Veterinary Medicine, University of Teramo, Campus Universitario Coste S. Agostino Via R. Balzarini 1, 64100 Teramo, Italy
[b] StemTeCh Group, Italy

ARTICLE INFO

Article history:
Received 24 June 2015
Received in revised form 25 November 2015
Accepted 19 January 2016

Keywords:
Amniotic epithelial cells
M1 macrophage
M2 macrophage
Ovine preclinical model
Tendinopathies
Regenerative medicine

ABSTRACT

Recently, we have demonstrated that ovine amniotic epithelial cells (oAECs) allotransplanted into experimentally induced tendon lesions are able to stimulate tissue regeneration also by reducing leukocyte infiltration. Amongst leukocytes, macrophages (Mφ) M1 and M2 phenotype cells are known to mediate inflammatory and repairing processes, respectively. In this research it was investigated if, during tendon regeneration induced by AECs allotransplantation, M1Mφ and M2Mφ phenotype cells are recruited and differently distributed within the lesion site. Ovine AECs treated and untreated (Ctr) tendons were explanted at 7, 14, and 28 days and tissue microarchitecture was analyzed together with the distribution and quantification of leukocytes (CD45 positive), Mφ (CD68 pan positive), and M1Mφ (CD86, and *IL12b*) and M2Mφ (CD206, *YM1* and *IL10*) phenotype related markers. In oAEC transplanted tendons CD45 and CD68 positive cells were always reduced in the lesion site. At day 14, oAEC treated tendons began to recover their microarchitecture, contextually a reduction of M1Mφ markers, mainly distributed close to oAECs, and an increase of M2Mφ markers was evidenced. CD206 positive cells were distributed near the regenerating areas. At day 28 oAECs treated tendons acquired a healthy-like structure with a reduction of M2Mφ. Differently, Ctr tendons maintained a disorganized morphology throughout the experimental time and constantly showed high values of M1Mφ markers. These findings indicate that M2Mφ recruitment could be correlated to tendon regeneration induced by oAECs allotransplantation. Moreover, these results demonstrate oAECs immunomodulatory role also in vivo and support novel insights into their allogeneic use underlying the resolution of tendon fibrosis.

1. Introduction

Tendon injuries are a common cause of disease and represent a significant health liability on society. Tendons can be exposed to trauma during sports activities, but they can also be affected by overuse or aging. The most commonly injured are Achilles and patellar tendons with pathologies ranging from degenerative tendinopathies, partial tears, up to complete ruptures (Jarvinen et al., 2005; Sharma and Maffulli, 2005; Duerden and Keeling, 2008). Horses suffer tendinitis of the superficial digital flexor tendon (SDFT), which is a significant cause of lameness and often a career-ending event in thoroughbred horses because of its high incidence, prolonged recovery period, and high rate of recurrence. These injuries are difficult to manage because tendons do not regenerate spontaneously, but originate a fibrotic scar with poor tissue quality and mechanical properties, frequently resulting in long-term pain, discomfort, and disability (Sharma and Maffulli, 2005; Sharma and Maffulli, 2006). Given the frequency and the increasing cost of treating injuries, as well as the relatively poor results obtained through surgical intervention, new and innovative cell-based therapies have become more appealing. Multipotent stem cells, termed tendon stem/progenitor cells (TDSCs/TSPCs), are present in tendons and ligaments (Bi et al., 2007; Ni et al., 2012), but they appear to be insufficient to sustain tendon regeneration in adults (Ruzzini et al., 2013). Moreover, the collection of TDSCs/TSPCs results very difficult for donor site morbidity (Ruzzini et al., 2013). Other stem/progenitor cells have been studied (Chong et al., 2009; Chen et al., 2011; Clarke et al., 2011; Young, 2012; Lange-Consiglio et al., 2013). In this context, in recent years amniotic-derived cells have attracted increasing attention as an alternative source of stem/progenitor cells for clinical application in regenerative medicine (Parolini et al., 2009; Malek and Bersinger, 2011; Miki, 2011; Barboni et al., 2012a; Mamede et al., 2012; Barboni et al., 2013; Colosimo et al., 2013; Murphy and Atala, 2013). In particular, ovine amniotic membrane-derived epithelial cells (oAECs) have been largely investigated for their regenerative tendon ability after allo-

* Corresponding author at: Faculty of Veterinary Medicine, Campus Universitario Coste S. Agostino Via R. Balzarini 1, 64100 Teramo, Italy.
E-mail address: vrusso@unite.it (V. Russo).

http://dx.doi.org/10.1016/j.rvsc.2016.01.014

(Muttini et al., 2010; Barboni et al., 2012a) or xeno-transplantation (Muttini et al., 2013) into experimentally induced tendon injuries. The results in Barboni et al. (2012a) demonstrated oAECs ability to support tendon regeneration with a prompt recovery of the biomechanical properties of the tissue. Indeed, in a previous paper (Barboni et al., 2012a) we have demonstrated that oAECs induced tendon regeneration through the modulation into the host tissue of crucial growth factors (i.e., VEGF and TGFβ1), and thanks to a large production of collagen type I (COL1) fibers deposited either by the recruited host tissue progenitor cells or directly by transplanted oAEC. In the host-injured tissue, some oAECs differentiated into tenocyte-like cells switching on, simultaneously, COL1 (Barboni et al., 2012a). In addition, oAEC allotransplantation promoted a specific and centripetal process of tissue regeneration that began close to the healthy portion of the tissue and then progressively invaded the core of the wound site, where oAECs rapidly migrated (Barboni et al., 2012a).

Amongst the crucial regenerating processes are anti-inflammatory/immunomodulatory effects (Parolini et al., 2009; Barboni et al., 2014; Magatti et al., 2014). Indeed, oAECs induced a reduction of leukocyte infiltration also in injured tendons (Barboni et al., 2012a). This AEC in vivo effect could be attributed to the innate immunomodulatory activities demonstrated in vitro (Parolini et al., 2008; Banas et al., 2008; Miki, 2011; Mattioli et al., 2012; Barboni et al., 2014) and could explain the use of these cells into allo- and xeno-transplantation settings (Cargnoni et al., 2009; Magatti et al., 2009; Barboni et al., 2012a; Muttini et al., 2013). However, the complex mechanisms involved in the in vivo immunoregulatory functions of AECs are not fully understood. The immunomodulatory effect on T and B lymphocytes (Barboni et al., 2014; Magatti et al., 2014) has been described, but new attention is now paid on their potential effects on macrophages (Mφ). Mφ play a crucial role in the resolution of tissue injury and promotion of tissue repair as described in several human diseases (Brancato and Albina, 2011). In response to chemotactic signals, monocytes migrate into tissues and subsequently differentiate into Mφ to replace aged ones or to participate in the initial phases of tissue defense in reaction to harmful insults (Murray and Wynn, 2011; Svensson et al., 2011). Mφ also play an essential role in the later phases of tissue homeostasis and repair phagocytazing apoptotic cells (Murray and Wynn, 2011). The origin and activation state of Mφ and their microenvironment are critical determinants of their response to injury. Functionally, Mφ can be polarized into distinct subpopulations, with specific functions related to the initiation and recovery phases of tissue injury (Murray and Wynn, 2011). Typically, Mφ are classified into two main groups: classically-activated Mφ (M1Mφ) and alternatively-activated Mφ (M2Mφ) (Gordon and Martinez, 2010; Murray and Wynn, 2011). M1Mφ are pro-inflammatory cells with potent anti-microbial activities and promote T helper 1 (Th1) cell responses and have also been implicated in many inflammatory diseases (Murray and Wynn, 2011). Conversely, M2Mφ are immunosuppressive cells that can support T helper 2 (Th2)-associated effector functions. M2Mφ are characterized by their low production of pro-inflammatory cytokines (i.e. IL1ß and IL12) and high production of anti-inflammatory cytokines (i.e. IL10) (Gordon and Martinez, 2010; Murray and Wynn, 2011). In particular, M2Mφ play a major role in the resolution of inflammation, tissue remodeling and wound repair by releasing IL10, secreting trophic factors and enhancing the clearance of apoptotic cells (Gordon and Martinez, 2010; Murray and Wynn, 2011).

Recent evidence starts to focus attention on Mφ-mediated mechanisms during cell-based preclinical approaches. Indeed, it has been shown that human placental mesenchymal stem cells (pMSCs) express their immunomodulatory role shifting M1 towards M2-like Mφ (Abumaree et al., 2013). In addition, human AEC-conditioned media altered bone marrow-derived Mφ polarization, migration, and phagocytosis, without affecting Mφ survival or proliferation in vitro. Similarly, hAECs mediated lung repair directly influencing Mφ behavior in a pro-reparative manner in vivo (Tan et al., 2014). In naturally occurring tendon injuries, Dakin et al. (2012) investigated the contribution of different Mφ subsets in an equine model. These authors have demonstrated that the pro-inflammatory M1Mφ predominated in sub-acute injury, whereas a potential phenotype-switch to M2Mφ polarity was seen in the chronic phase of injury (Dakin et al., 2012).

Based on the assumption of the crucial role of Mφ population in tissue resolution described in the literature, the present research was designed to investigate Mφ infiltration after oAECs allotransplantation into a validated preclinical tendon regenerative model (Barboni et al., 2012a). In particular, it was investigated if pro-inflammatory M1Mφ and pro-regenerative M2Mφ phenotype were recruited and if they were differently distributed within the lesion site during the early phases of the repair process induced by oAECs allotransplantation. The experiments were carried out on an ovine model chosen for its high translational value for musculoskeletal regenerative horse and human pathologies (Wagner and Storb, 1996; Bruns et al., 2000; Wang, 2006; McCarty et al., 2009).

2. Materials and methods

2.1. Ethic statement

The Ethical Committee CEISA of the University of Chieti and Teramo has approved all experimental procedures (approval ID 27/2010/CEISA/COM of 11/11/2010). Eighteen Appenninica breed sheep, two years old with a mean weight of 40 kg, were used. The sheep were bred according to the European community guidelines (E.D. 2010/63/UE) before performing bilateral tendon lesions. Animals were quarantined for 2 weeks to check the general healthy status. Surgical procedures were carried out under general anesthesia and in an authorized veterinary hospital. The animals were randomly divided into three groups and euthanized to explant grafted tendons at 7, 14, and 28 days. Animals were euthanized by applying an overdose of thiopental (Pentothal Sodium, Intervet) and embutramide (Tanax®, Intervet).

2.2. Ovine AECs isolation and labeling

Ovine AECs (oAECs) were collected from slaughtered sheep of Appenninica breed at 3 months of pregnancy (25–30 cm of length). The cells were obtained from the isolated amniotic epithelial layer after enzymatic digestion (Trypsin–EDTA, Sigma Chemical Co., St. Louis, MO, USA) as previously described by Barboni et al. (2012a). Briefly, cell suspensions were seeded in flasks in minimum essential medium Eagle-α modification (α-MEM) supplemented with 20% fetal calf serum (FCS), 1% ultraglutamine, 1% penicillin/streptomycin plus 10 ng/ml epidermal growth factor (EGF) at a concentration of 3×10^3 cells/cm^2. At 70% confluence, the cells were dissociated by 0.05% trypsin–EDTA and frozen in α-MEM containing 20% FCS and 10% dimethyl sulfoxide (DMSO). Thawed cells were plated again at 3×10^3/cm^2 for three consecutive passages. Ovine AEC morphology during the in vitro culture was analyzed with an inverted microscope, whereas Cytokeratin 8 expression was evaluated using the monoclonal anti-Cytokeratin 8 primary antibody (1 μg/ml; Abcam, Cambridge, UK) and an anti-mouse Alexa Fluor 488 (2 μg/ml; Invitrogen Ltd., Paisley, UK) secondary antibody for its retrieval by immunocytochemistry as described in our previous report (Barboni et al., 2012b). The proliferative activity was analyzed by calculating in triplicate oAECs doubling time (total number of cells/plate every 24 h) starting from day 0 to day 4 of culture. oAEC molecular characterization were performed by flow cytometry investigations, as previously described in our reports (Mauro et al., 2010; Barboni et al., 2012a; Mattioli et al., 2012; Barboni et al., 2014) for haemopoietic markers (CD14, CD58, CD31 e CD45), surface adhesion molecules (CD29, CD49f and CD166), stem cell markers (TERT, SOX2, OCT4, NANOG), for MHC class I molecule and MHC class II (HLA-DR) antigens. Details of specific antibodies used and flow cytometry procedures have been previously described

Table 1
Antibodies used for IHC.

Primary abs		Secondary abs	
	μg/ml		μg/ml
CD45 (AbD Serotec, Oxford, UK)	0.5	Anti-mouse-FITC (Sigma-Aldrich, Missouri,USA)	5
CD68 (Dako, Glostrup, Denmark)	5	Anti-mouse Alexa Fluor 488 (Invitrogen Ltd., Paisley, UK)	2
CD86 (Serotec, Gibbstown, NJ)	0.02	Anti-mouse Alexa Fluor 488 (Invitrogen Ltd., Paisley, UK)	5
CD206 (R&D System Cambridge, UK)	4	Anti-mouse FITC (Sigma-Aldrich, Missouri,USA)	5
COL1 (Chemicon Int. Billrerica, USA)	1	Anti-mouse Alexa Fluor 488 (Invitrogen Ltd., Paisley, UK)	2

(Mauro et al., 2010; Barboni et al., 2012a; Mattioli et al., 2012; Barboni et al., 2014). Then, 2.5×10^6 oAECs were stored in liquid nitrogen in vials. Before transplantation, thawed oAECs were stained with the red fluorescent cell linker dye PKH26, according to manufacturer's instructions (Sigma) as previous described (Barboni et al., 2012a and Barboni et al., 2012b; Muttini et al., 2013; Barboni et al., 2013). The PKH26 dye stably incorporates into lipid regions of the cell membrane. Due to this extremely stable fluorescence, PKH26 is the linker dye of choice for in vivo cell tracking and monitoring studies (http://www.sigmaaldrich.com/technical-documents/articles/biowire/cell-tracking.html; https://www.sigmaaldrich.com/content/dam/sigma-ldrich/docs/Sigma/Bulletin/mini26bul.pdf).

Briefly, thawed oAECs cells were re-suspended in 1 ml of Diluents C and then added at 1 ml of Dye Solution containing 4 μl of PKH26. The cellular suspension was incubated for 5 min at room temperature with periodic mixing. Cells staining was stopped with 2 ml of 1% PBS/BSA for 1 min and finally centrifuged at 400 $\times g$ for 10 min. Cells were suspended and counted in order to obtain 4×10^6 PKH26–marked oAECs vital cells to be used for transplantation.

2.3. Surgical procedure and oAECs transplantation technique

The experimental surgical procedure was performed as previously described by Barboni et al. (2012a). Under general anesthesia, the pelvic limbs of the animals were placed off with both tarsi under flexion. A 3 cm skin incision was made, starting at 4 cm proximal to the *tuber calcis*. The medial and more prominent component of the Achilles tendon, that is, the tendon of *m. flexor digitorum superficialis*, was isolated. Using a sterile punch, a full thickness hole, 3 mm in diameter, was realized. Using a randomized pattern, the lesion of one limb was filled with a total volume of 30 μl composed of a suspension containing 4×10^6 oAECs-PKH26 labeled cells plus fibrin glue (1:1, v/v; Tissucol; Baxter Spa) (oAECs treated tendon), while the contralateral lesion was filled with fibrin glue alone (Ctr tendon) (Awad et al., 2003; Hoffmann et al., 2006; Hou et al., 2009a and Hou et al., 2009b; Barboni et al., 2012a). The paratenon and fascia were closed before skin suture. After surgery animals were kept in a small holding corral until sacrifice. Animals and surgical wounds were inspected daily. Eighteen animals were randomly divided amongst the three time points, 7, 14, and 28 days, in order to process the tendon explants, Ctr and oAEC treated tendons, for the morphological and molecular analyses. Animals were euthanized by applying thiopental (Pentothal Sodium, Intervet) and embutramide (Tanax®, Intervet).

2.4. Morphological and immunohistochemical analysis

Ctr and oAECs explanted tendons at 7, 14, and 28 days after transplantation, were transversally cut at least 5 mm from the injured area. The specimens were placed in liquid nitrogen. Cryosections, 7 μm in thickness, were processed with hematoxylin–eosin (H&E) and immunohistochemistry (IHC) as described in our previous report Barboni et al. (2012a). H&E stain was carried out to obtain information on the tissue cell concentration, microarchitecture regeneration and extracellular matrix reorganization, within the injured tendons during the different interval points (7, 14, and 28 days) using a scoring system as previously reported in Barboni et al. (2012a) slightly modified. Three different scores were adopted to indicate:

- Score 1, a damaged tissue with cells showing rounded nuclei, and a faint disorganized extracellular matrix;
- Score 2, an early stage of tendon healing showing cells with rounded nuclei, an increased matrix deposition with fibers acquiring a parallel orientation;
- Score 3, an early stage of tendon regeneration with prevalent flat shaped cells and fusiform nuclei, an extracellular matrix characterized by oriented fibers along the longitudinal axis of the healthy tendon.

The IHC analyses were performed with the antibodies:

- monoclonal mouse anti sheep COL1 (Barboni et al., 2012a, 2012b) in order to evaluate collagen Type I fiber deposition;
- monoclonal mouse anti sheep CD45 (MCA2220F) (Barboni et al., 2014) in order to evaluate pan leukocytes;
- monoclonal mouse anti-human CD68 (clone EBM11) (Di Palma et al., 2012) in order to evaluate pan Mφ infiltrations;
- monoclonal mouse anti-bovine CD86 (MCA2437GA, clone IL-A190) (Neeland et al., 2014) in order to evaluate specific pro-inflammatory M1Mφ cells;
- Polyclonal Goat IgG anti-human MMR/CD206 (AF2534) (Kuo et al., 2011) in order to evaluate anti-inflammatory M2Mφ cells.

Detailed information on primary antibodies and on secondary antibodies used for their retrieval are summarized in Table 1. Cell nuclei were identified with DAPI. Primary antibodies were replaced with non-immune sera as negative controls.

2.5. Morphometric analysis

Morphometric analyses were performed with an Axioscop 2plus epifluorescence microscope (Zeiss, Oberkochen, Germany) equipped with a cooled color charge-coupled device camera (CCD; Axiovision Cam, Zeiss) interfaced with an interactive and automatic image analyzer (Axiovision, Zeiss). The data were processed using a KS300 computed image analysis system (Zeiss) and quantified as previously described (Barboni et al., 2012a). Briefly, guided programs (macros for KS300) were created to count inside a standard area of 20,000 μm^2: cell presence (total number of DAPI stained nuclei in the area), leukocyte infiltration (% CD45-positive cells/total number of nuclei in the area), Mφ infiltration (% CD68-positive cells/total number of nuclei in the area), pro-inflammatory M1Mφ phenotype population (% CD86-positive cells/total number of nuclei in the area), and anti-inflammatory M2Mφ phenotype populations (% CD206-positive cells/total number of nuclei in the area). Analyses were carried out on at least five different

sections of each tendon specimen analyzed (total tendon analyzed/group = 5). Morphometric analyses were performed at 200× magnification by capturing five images from six contiguous areas starting from the healthy zone (area 0) and proceeding throughout the repairing zones for five consecutive areas (areas 1–5). The extension of each zone analyzed was ~300 μm and, therefore, the total area analyzed within each section was ~1800 μm (Barboni et al., 2012a).

Sections with retrieved PKH26-positive cells were immunostained, as described above, for CD86 and CD206. Morphometric analyses were adopted to evaluate the percentage of PKH26-positive cells that co-localized with CD86 or with CD206 (CD86 or CD206 and PKH26 double-stained cells/total number of PKH26 cells). The morphometric analyses were performed on at least five fields on all the consecutive sections that displayed engrafted PKH26-positive cells.

2.6. Laser capture micro dissection (LCM) technique

Procedures for LCM were performed as previously reported in Barboni et al. (2012a). Briefly, the frozen sections were air-dried on uncoated glass slides and washed with 70% ethanol. The sections were kept on dry ice at −80 °C until they were subjected to LCM. Just before the procedure, the sections were fixed in 70% ethanol for 10 s and stained with H&E according to Hoffmann et al. (2006). LCM were performed by using a Laser Capture Micro dissection (MMI Cellcut device) apparatus. The settings of the laser were performed as follows: spot diameter 10 μm, pulse duration 50 ms; laser power 50 mW. The areas to micro-dissect were identified under a light microscope at ×40 of magnification including a portion of the implantation site within the host tendon. Every section was dropped on a separate cap. Micro-dissected sections (n = 30 sections)/sample were immediately processed for RNA extraction and RT-PCR procedures.

2.7. RNA isolation and RT-PCR procedures

Total RNA was extracted from tendon micro-dissected cryosections (n = 30 for each animal group/time) by TriReagent (Sigma) following manufacturer's instruction as previous reported in Barboni et al. (2012a). Agarose gel electrophoresis (1%) and ethidium bromide staining was used to evaluate RNA integrity. The RNA was treated with DNaseI digestion (Sigma) for 15 min at RT. Total RNA (1 μg) of each sample was used for reverse transcription reaction with the Oligo dT primer and BioScriptTM (Bioline). 2× ready mixTM Taq PCR reactions mix (Sigma) was used for PCR reaction using 3 μl of cDNA and 0.5 μM of each primer in a final volume of 25 μl. The PCR gene primers, mRNA sequence GenBank number, product length, and cycles are shown in Table 2. The reaction mixtures were incubated for 5 min at 95 °C, followed by 95 °C for 30 s, 55 °C for 30 s, 72 °C for 45 s, and 72 °C for 7 min. RT-PCR was normalized by the transcriptional levels of glyceraldehyde 3-phosphate dehydrogenase (GAPDH). The PCR products were separated on 2% agarose gel stained with ethidium bromide, visualized on a Gel Doc 2000 (Biorad), and analyzed with Quantity One 1-D Analysis software (Biorad). Each reaction was carried out in triplicate.

Table 2
Primer sequences used for RT-PCR.

Gene	Accession no.	Primer sequences	Size (bp)	Cycles
CD86	AY395982.3 Ovine	F: AGAAGGTCCCAAGGACTGGT R: GCTTGGCACAGGTGACTTTG	387	40
CD206	NM001197180.1 Ovine	F: GTAGAAGCAGGCTGCCAGAA R: CTTCTGCCCAGTGTTTGCAC	394	40
YM1	XM004013541.1 Ovine	F: AGGACATCATAGCCCCCTGT R: GCTCCGTGGAGGAAATCACA	270	40
IL10	NM001009327.1 Ovine	F: CTGTGCCTCTCCCCTAGAGT R: GCAGCTAGCTCCACAAGGAA	237	40
IL12b	NM001009438.1 Ovine	F: ACAAAGGAGGCGAGGTTCTG R: CTGTGGTCCATGCTGACCTT	283	40
GAPDH	AF030943.1 Ovine	F: CCTGCACCACCAACTGCTTG R: TTGAGCTCAGGGATGACCTTG	224	40

2.8. Statistical analysis

The quantitative data obtained, expressed as mean ± Standard Error (±SE), were firstly assessed for distribution by D'Agostino and Pearson tests. Data sets were compared using ANOVA tests followed, when necessary, by posthoc Tukey tests (GraphPad Prism 5, GraphPad Software, USA). The values were considered statistically significant for $p < 0.05$.

3. Results

3.1. oAECs culture, characterization and stain

According to our previous studies (Barboni et al., 2012a; Mattioli et al., 2012; Muttini et al., 2013) ovine AECs showed, in in vitro culture, a typical polyhedral phenotype characterized by the cytokeratin 8 epithelial marker expression (Fig. 1A). Cells proliferated with an average doubling time of 20–24 h and, showed the molecular profile indicated, by the flow cytometry analysis (Fig. 1A). oAEC did not display any haemopoietic markers (CD14, CD58, CD31 e CD45). On the contrary, the cells expressed several surface adhesion molecules (CD29, CD49f and CD166), and the stemness markers TERT, SOX2, OCT4 and NANOG, while the CD117 resulted not expressed (Fig. 1A). Cells maintained all characteristics until third passage in culture also after freezing and thawing cycles (Fig. 1A). The thawing procedures did not influence cell vitality because oAECs remained healthy and were able to incorporate the vital PKH26 red stain before transplantation (Fig. 1Ba). Cells maintained the dye both in in vitro (Fig. 1Bb) and in in vivo (Fig. 1Bc) experiments. Indeed, in explanted oAEC treated tendons the recovery of red PKH26-labeled oAECs with healthy nuclei indicate their stable integration in the tissues up to 28 days after transplantation (Fig. 1Bc).

3.2. Microarchitecture tendon recovery

The tendon lesion site and PKH26-labeled oAECs injection procedures were performed using a validated experimental technique (Barboni et al., 2012a). Tendons were explanted at 7, 14 and 28 days after transplantation. The defect area in tendon explants was macroscopically detected as a circle/irregular hemorrhagic zone localized in the middle portion except in oAEC treated tendons at day 28 where it appeared as a white opalescent zone with few hemorrhagic signs (data not shown). The differences between Ctr and oAECs tissue microarchitecture began to be evident at day 7 (Fig. 2Aa and Ad). In particular, tendon cell nuclei were entrapped within a still evident fibrin glue in Ctr (score 1, Fig. 2Aa), and into a faint and irregularly organized extracellular matrix in oAEC treated tendons (score 1, Fig. 2Ad). The tissue remodeling progressed rapidly in the presence of oAECs. At day 14, a greater matrix deposition with fibers acquiring a parallel orientation and a prevalent presence of fusiform cell nuclei (score 2, Fig. 2Ae) were recorded. At day 28, a higher extracellular matrix density and oriented fibers became evident within the healing area (score 3, Fig. 2Af). On the contrary, rounded nuclei enclosed within a disorganized extracellular matrix persisted into the wound area of Ctr tendons until day 28 (score 1, Fig. 2Ab and 2A c). According to our previous report (Barboni et al., 2012a), COL1 was almost absent in the lesion site of both tendons at day 7 and started to be present in oAECs treated tendons after 14 days (data not shown). Then, after 28 days, COL1 was expressed in allotransplanted sites as fiber-like wires presenting a density and orientation along the longitudinal axis of the tendon similarly to the healthy portion of the tissue (Fig. 2Bb). On the contrary, COL1

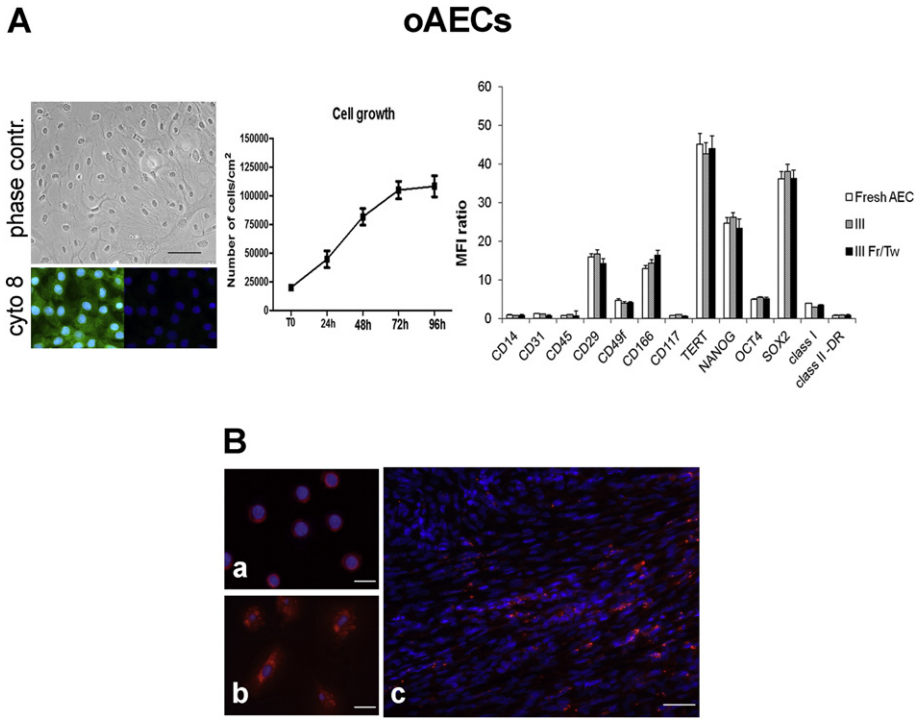

Fig. 1. Molecular characterization of cultured and cryopreserved oAECs. (A). Representative images of in vitro cultured oAECs displaying a polyhedral phenotype (phase contrast) and cytokeratin 8 positivity (green color). Nuclei were counterstained with DAPI (blue color). Scale Bar: 50 μm for all images. oAECs growth curve was established calculating the rate of growth of cells every 24 h for 4 days (values are mean ± SD of 3 different experiments). The histogram indicates the molecular profile of surface, MHC and pluripotency markers expressed as Mean Fluorescence Intensity (MFI) ratio (values are mean ± SD of 3 different biological samples) levels obtained with flow cytometry analysis. All analyses were carried out on oAECs expanded in vitro for III passages, before and after freezing and thawing (Fr/Tw). (B). Representative images of PKH26-labeled oAECs (red color) after thawing and labeling before transplantation (a), in in vitro culture after thawing and labeling (b) and in explanted tendons after 28 days transplantation (c). Nuclei were counterstained with DAPI (blue color). Scale bar: 20 μm, 25 μm and 50 μm, respectively.

was absent at 14 days (data not shown) and barely detectable in Ctr tendons at day 28 displaying a scattered random distribution throughout the repairing site (Fig. 2Ba).

3.3. Cell, leukocyte and macrophage infiltration during tendon healing

The morphometric analysis of cell (Fig. 3A), leukocyte (Fig. 3B) and macrophage infiltration (Fig. 3C) in Ctr and oAEC treated tendons was carried out on tissue sections divided in six contiguous areas, from the healthy zone (area 0) up to the core of the lesion (area 5), at 7, 14, and 28 days after transplantation. PKH26-labeled oAECs were always identified inside the defect area with a distribution that was strictly dependent on the progression of tissue healing. At day 7, oAECs rapidly migrated towards the healthy portion of the tissue in the areas 1 and 2 (arrows in Fig. 3A). Then, they were recorded at day 14 into the areas 3–4, and at day 28 into the areas 4–5 (arrows in Fig. 3A).

Cellularity in oAEC treated tendons was significantly higher in the areas 1–2 at day 7 (Fig. 3A, $p < 0.05$), and in the areas 4–5 (Fig. 3A; $p < 0.05$) at day 14. Then, cellularity decreased at day 28 becoming significantly lower in areas 2–4 than in Ctr (Fig. 3A, $p < 0.05$).

Inflammatory cell infiltration was evaluated using an anti CD45 antibody, a pan leukocyte marker (Fig. 3B), an anti CD68 antibody, a pan Mφ marker (Fig. 3C). CD45-positive cells were significantly lower in oAEC treated tendons at day 7 in the whole defect area, areas 1–5, (Fig. 3B, $p < 0.05$) than in Ctr. Then, the percentage of leukocytes were similar to the ones of the healthy portion of the tissue and significantly lower than in Ctr at day 14 in the areas 1–4, and at day 28 in the areas 3–5 (Fig. 3B, $p < 0.05$). The percentage of CD68-positive cells was similar between Ctr and oAEC treated tendons at day 7 (Fig. 3C, $p > 0.05$). On the contrary, at day 14 and 28 it was lower in allotransplanted tissues than Ctr ones in most of the areas (Fig. 3C, $p < 0.05$).

3.4. M1Mφ and M2Mφ related gene expression during tendon healing

In order to study the activation state of the Mφ during the early phase of tendon healing, the expression of *CD86*, *IL12b* genes associated with pro-inflammatory M1Mφ and *CD206*, *IL10*, *YM1* genes associated with anti-inflammatory and pro-reparative M2Mφ phenotype was determined by RT-PCR (Fig. 4 and Fig. 5).

As summarized in Fig. 4, a progressive reduction of *CD86* mRNA expression was recorded in oAEC treated tendons. In detail, at day 7, *CD86* mRNA levels were similar in both tendons to significantly decrease at day 14 and 28 only in oAEC treated tendons, whereas in the Ctr it remained stable on high values during the early phase of healing (Fig. 4A and B, $p < 0.05$). Moreover, *IL12b* mRNA expression was always significantly lower in oAEC treated tendons and even undetectable at day 28 (Fig. 4A and B, $p < 0.05$). In Ctr tendons, a significant reduction of *IL12b* mRNA levels was exclusively observed at day 28 (Fig. 4A and B, $p < 0.05$).

At day 7, *YM1*, *CD206* and *IL10* were similarly expressed (Fig. 5A). At day 14, *CD206* and *YM1* mRNA increased in both groups even if they reached higher levels in oAEC transplanted tissues (Fig. 5B, $p < 0.05$). On the contrary, at day 14 *IL10* mRNA level strongly increased exclusively in the presence of oAECs (Fig. 5B, $p < 0.05$). At day 28, the expression of both *CD206* and *IL10* decreased in oAEC treated tendons which was similar to the one observed in Ctr tendons. At this time, *YM1* mRNA level appeared to be significantly lower in oAEC treated tendons than in the Ctrs (Fig. 5B, $p < 0.05$).

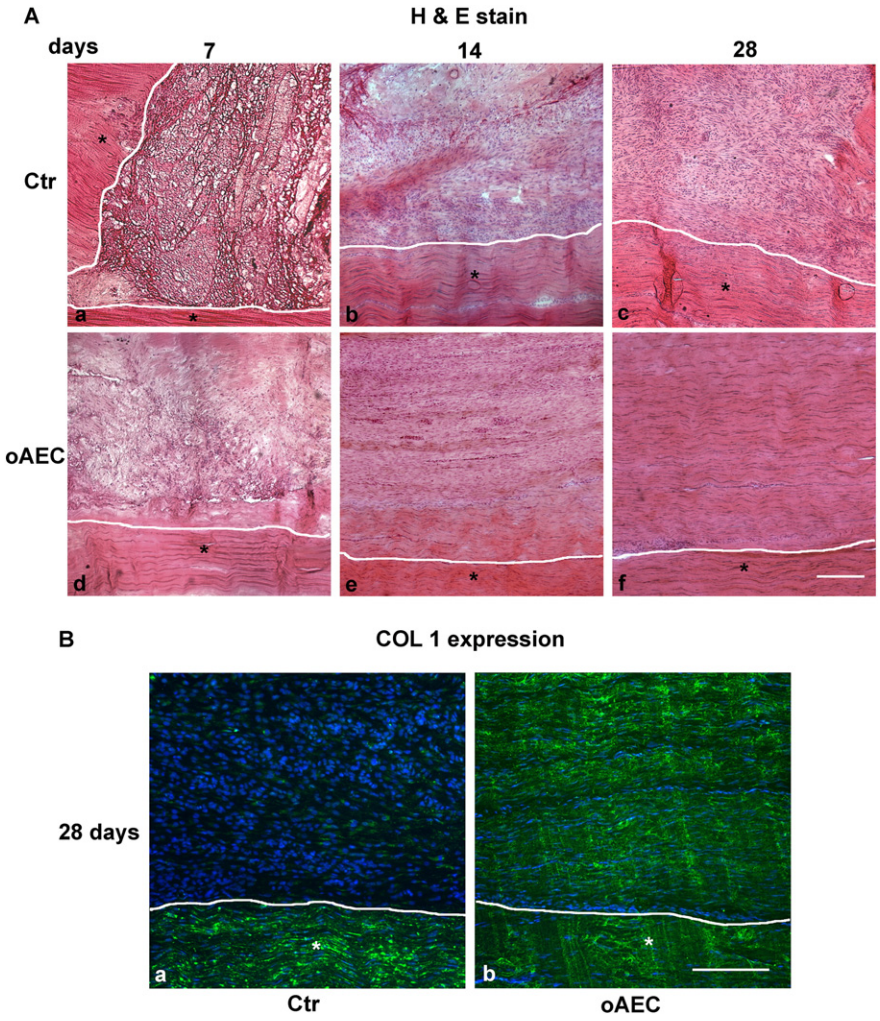

Fig. 2. Morphological analysis of tendon healing. (A). H&E stain of injured Achilles tendon performed at 7, 14, and 28 days post treatment in Ctr (a–c) and oAEC treated tendons (d–f). The healing portion and the healthy portion (asterisk) of tendon tissue are above and below the white line of the pictures, respectively. The images show a faster tissue organization in oAEC treated tendons than in Ctr ones. oAECs, tendon allotransplanted with amniotic epithelial cells; Ctr, contralateral tendon treated with only fibrin glue; H&E, hematoxylin and eosin staining. Scale bar: 250 μm for all the images. (B). representative IHC images of COL1 (green color) expression performed at 28 days post treatment in Ctr (a) and oAEC treated tendons (b). The images show a COL1 deposition and alignment in oAEC treated tendons respect to Ctr ones where COL1 expression is barely detectable. Nuclei were counterstained with DAPI (blue color). Scale bar: 120 μm for all the images.

In order to determine whether the macrophage population was balanced towards M1 to M2 phenotype, the ratio of *IL12b* to *IL10* was also considered. The lower *IL12b*:*IL10* ratio in oAEC treated tendons confirmed a skewing towards M2Mφ phenotype during the early phase of healing (Fig. 5B).

3.5. M1Mφ and M2Mφ tissue distribution during tendon healing

The presence and distribution of M1Mφ and M2Mφ subpopulations were evaluated within the lesion site. In particular, the IHC analysis was carried out to quantify and identify the pro-inflammatory M1Mφ phenotype (Fig. 6A–B) using the CD86 marker, whereas the pro-reparative M2Mφ phenotype using the CD206 marker (Fig. 6C–D).

At day 7, M1Mφ infiltration was particularly high in the entire defect zone of oAEC treated tendons (Fig. 6A). At day 14, the percentage of CD86 positive cells dropped in oAEC treated tendons (Fig. 6A, $p < 0.05$). Several CD86 positive cells (green marked) were recorded close to several PKH26 (red marked) labeled cells (Fig. 6B: central and bottom images) in the areas 3–4. Approximately 10% of them co-localized with the PKH26 dye assuming a yellow merged fluorescence (Fig. 6C: arrows bottom image). Most of the M1Mφ were localized in the area 5 (Fig. 6A). Differently, in Ctr tendons the percentage of CD86 positive cells was always higher (Fig. 6A, $p < 0.05$), and evenly distributed within the lesion site (Fig. 6C: top image). At day 28, the percentage of M1Mφ in allotransplanted tendons further decreased reaching values similar to those recorded into the healthy portion of the tendon. At this time, the percentage of M1Mφ cells co-localizing with the red fluorescence increased to ~35% of oAEC-PKH26 labeled cells. The percentage of CD86 positive cells in Ctr tendon at day 28 resulted still significantly higher reaching values of approximately 20% in the whole defect area (Fig. 6A, $p < 0.05$).

M2Mφ subpopulation, identified by the CD206 marker, displayed a different behavior in oAEC treated and Ctr tendons. At day 7, the infiltration of M2Mφ was evident in the entire defect zone of both allotransplanted and Ctr tendons (Fig. 6C). At this time, the percentage of CD206 positive cells did not change in Ctr tissues (Fig. 6C), whereas it significantly raised in the areas 2–3 of oAEC treated ones (Fig. 6C, $p < 0.05$). The M2Mφ cells localized in the areas 2–3 were recorded close to the PKH26 positive cells and never co-localized the PKH26 red fluorescence (Fig. 6D: central and bottom images). At day 28, the

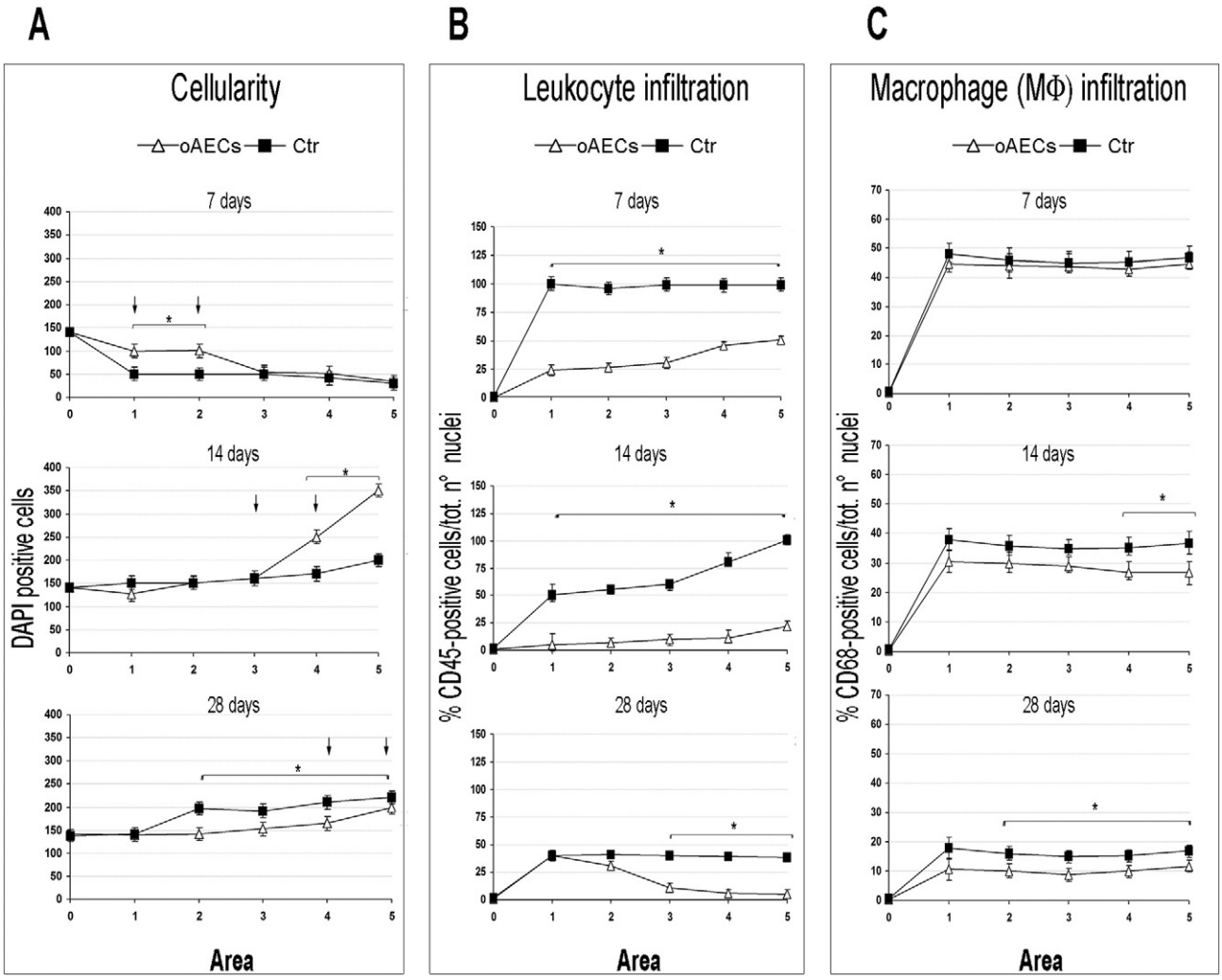

Fig. 3. Spatio-temporal modification of leukocyte and macrophage infiltration. Quantification of (A) cellularity, (B) leukocyte and (C) macrophage infiltration in healing tendons performed at 7, 14, and 28 days post treatment. The data are presented as median ± 25° and 75° percentile of 15 determinations/area/animal performed at 200× of magnification by capturing five images from six contiguous areas (indicated on x-axis as 0–5) starting from the healthy portion of the tissue (area 0) and proceeding throughout the repairing area (1–3) to the core of the lesion (4–5). Each area analyzed was ~300 μm for an overall length of ~1800 μm. The final data considered for each time point are the median of 90 different determinations (15 determination/area for 6 different animals/time point). Arrows indicated oAECs localization within the areas. *Significantly different values between Ctr and oAECs treated tendon. oAECs, transplanted tendons with amniotic epithelial cells; Ctr, contra lateral tendon treated with only fibrin glue; cellularity, expressed as the total number of nuclei (DAPI stained) in the area; leukocyte infiltration, expressed as percentage of CD45 positive cells/total number of nuclei in the area; macrophage infiltration, expressed as percentage of CD68 positive cells/total number of nuclei in the area.

percentage of M2Mφ was significantly lower in oAEC treated tendons in areas 1–4 (Fig. 6B, $p < 0.05$) whereas it remained on high levels in the core of the lesion (area 5, Fig. 6C).

4. Discussion

The present study demonstrates, for the first time, that macrophages M1 and M2 phenotypes are recruited and differently distributed during the early phase of tendon regeneration induced by oAECs allotransplantation in an ovine tendon defect model with respect to Ctr tendons. In particular, the presence of pro-regenerative M2Mφ phenotype subpopulations was strictly correlated to oAECs ability to induce tissue regeneration. This result allows us to speculate their immunomodulatory properties also in an in vivo model, as it was already demostrated in vitro (Barboni et al., 2014). Indeed, differently from Ctr tendons, oAEC treated tendons showed a reduction of pro-inflammatory M1Mφ, and the simultaneous recruitment of pro-regenerative M2Mφ phenotype in the lesion site. This modulation on M1Mφ and M2Mφ subpopulations was temporally related to the recovery of tissue microarchitecture recorded in allotransplanted oAEC treated tendons. Similarly to lung model repairing after bleomycin-induced injury model (Cargnoni et al., 2009; Moodley et al., 2010; Murphy et al., 2011; Vosdoganes et al., 2013; Tan et al., 2014) or to hepatic fibrosis resolution after CCL4 administration (Manuelpillai et al., 2012), also oAECs allotransplantation in a tendon injury model could be involved in Mφ polarization. It is reasonable to hypothesize that during tendon healing, oAECs exhibit pleiotropic immune regulatory activities, which are mediated by complex mechanisms involving a spatial factors secretion that inhibit the recruitment of leukocytes and the in situ activation/polarization of Mφ subpopulations. The recent immunomodulatory properties of oAECs observed in vitro (Barboni et al., 2014) could explain the in vivo oAECs allotransplantation effects. A conserved ability to inhibit lymphocyte proliferation either in transwell co-culture or in cell-to-cell contact systems was demonstrated in vitro (Barboni et al., 2014; Magatti et al., 2014). However, in this research the in vivo oAECs immunomodulatory property could be also strictly addressed to macrophage recruitment, resulting an in situ activation of alternative M2Mφ, and a simultaneous inhibition of classically M1Mφ phenotype during the

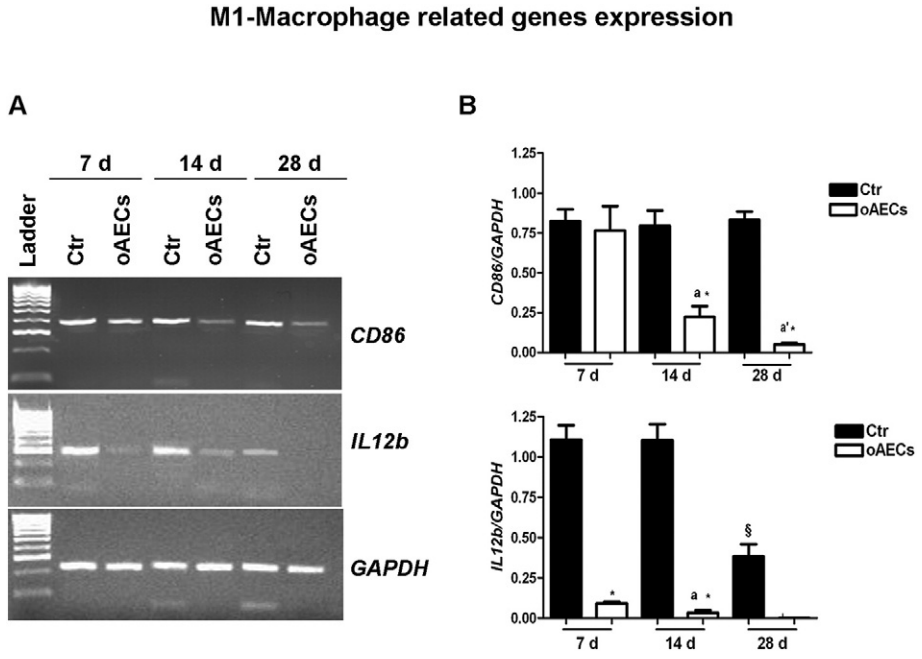

Fig. 4. M1 macrophage related gene expression profile in the defect area of healing tendons. (A) An example of RT-PCR images of *CD86* and *IL12b* mRNA expression in Ctr and oAEC treated tendons performed at 7, 14, and 28 days (d) post treatment. (B) Semiquantitative analysis normalized for GAPDH (values are mean of 3 replicates ± SD). [§]Significantly different values in the Ctr tendons during the different time points ($p < 0.05$); [a a']Significantly different values in the oAEC treated tendons during the different time points ($p < 0.05$); *Significantly different values between Ctr and oAEC treated tendons within each time point ($p < 0.05$).

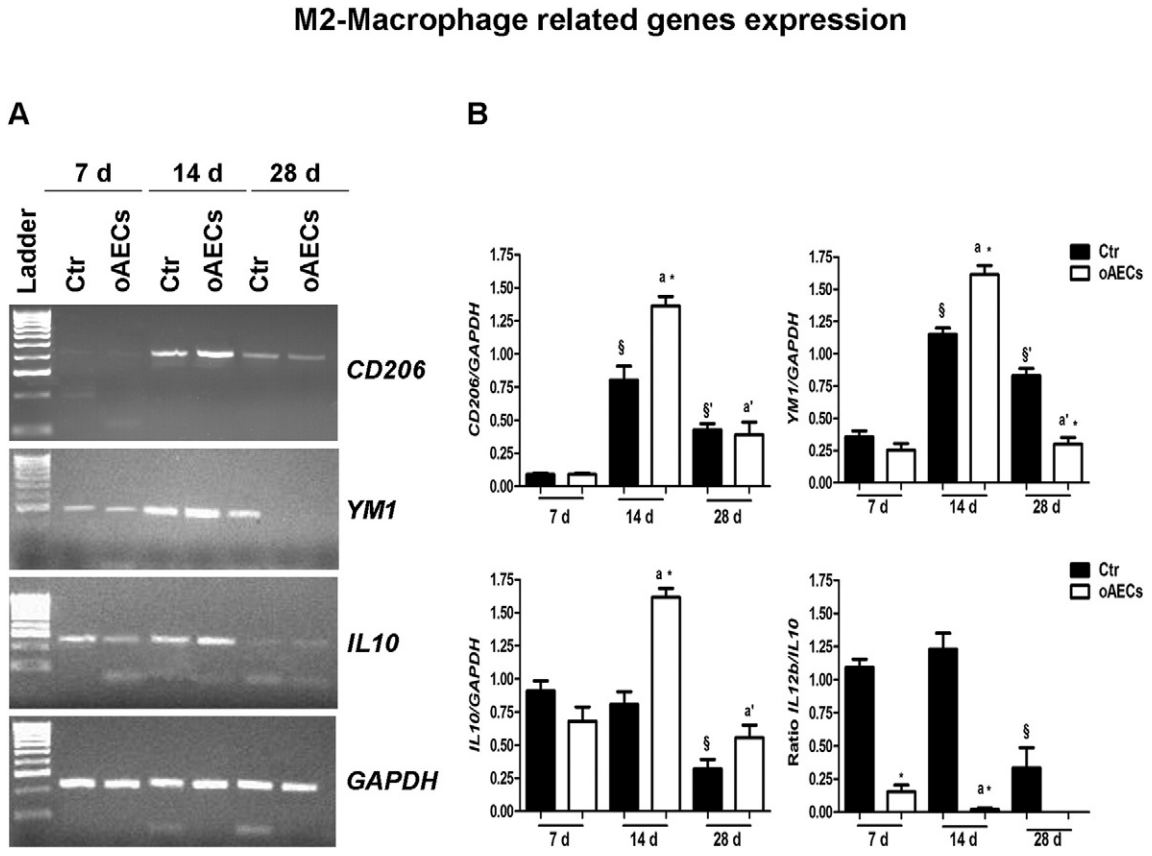

Fig. 5. M2 macrophage related gene expression profile in the defect area of healing tendons. (A) An example of RT-PCR images of *CD206*, *YM1* and *IL10* mRNA expression performed at 7, 14, and 28 days (d) post treatment. (B) Semiquantitative analysis of genes normalized for *GAPDH* (values are mean of 3 replicates ± SD). Ratio *IL12b*/*IL10* indicated temporal skewing form M1 to M2 macrophages during the healing process. [§, §']Significantly different values in the Ctr tendons during the different time points ($p < 0.05$); [a, a']Significantly different values in oAEC treated tendons during the different time points ($p < 0.05$); *Significantly different values between Ctr and oAEC treated tendons within each time point ($p < 0.05$).

early phases of tendon healing. oAECs migration into the tendon defects seemed to be essential to drive the centripetal progression of tendon healing and Mφ recruitment/activation. In fact, we have previously demonstrated that tendon regeneration induced by oAECs begins from the healthy portion of the tissue to invade progressively the core of the wound site where the allotransplanted oAECs actively migrate (Barboni et al., 2012a). Indeed, oAECs were always recorded close to the front side of tissue regeneration contributing to growth factor, such as VEGF and TGFβ1, and cytokine paracrine secretion. These molecules induced host cell proliferation, blood vessel remodeling, and collagen neo-deposition positively influencing the newly deposited extracellular matrix organization and its orientation along the longitudinal axis of the healthy tendon (Barboni et al., 2012a; Muttini et al., 2013). Overall, these events led to an early tissue microarchitecture recovery of the injured tendon with a significant improvement of its biomechanical-proprieties (Barboni et al., 2012a). Tissue remodeling was also supported by a direct oAEC trans-differentiation into tendon like cells (Barboni et al., 2012a; Muttini et al., 2013). In the present research when oAEC treated tendons began to recover their microarchitecture, a simultaneous reduction of pro-inflammatory M1Mφ markers, mainly distributed close to AECs, and a drastic increase of pro-regenerative M2Mφ markers, localized near the regenerating areas, was evidenced, allowing to speculate an additional oAEC paracrine effect towards the host tissue involving Mφ recruitment. The importance of a local Mφ polarization during wound healing and tissue regeneration is largely documented (Ariel et al., 2012; Gautier et al., 2012; Manuelpillai et al., 2012; Abumaree et al., 2013; Davies et al., 2013; Labonte et al., 2014; Tan et al., 2014). Even if the mechanisms involved remain partially unknown, it has been widely recognized that the secretion of anti-inflammatory cytokines and collagen degrading enzymes from Mφ are frequently involved in tissue repair (Wynn and Barron, 2010). Moreover, M2Mφ recruitment dependent on AECs transplantation, has been recognized as a crucial anti-inflammatory and anti-fibrotic mechanism that supports lung and hepatic tissue repair (Cargnoni et al., 2009; Manuelpillai et al., 2012; Abumaree et al., 2013; Tan et al., 2014). Anti-inflammatory M2Mφ are polarized by specific interleukins (IL4, IL10 and IL13) (Mosser and Edwards, 2008; Labonte et al., 2014) some of them secreted in appreciable amounts by fetal membranes (Williams et al., 2000; Bowen et al., 2002). Instead, the pro-inflammatory M1Mφ are usually stimulated during the acute phase of inflammation in response to interferon gamma IFNγ alone or in combination with microbial or cytokines stimuli (e.g. Tumor necrosis factor α) (Mosser and Edwards, 2008). Indeed, a massive presence of pro-inflammatory M1Mφ subpopulation was observed at day 7 both in oAEC treated and in Ctr tendons suggesting an ongoing inflammatory state. However, starting from day 14, oAECs reduced the presence of pro-inflammatory M1Mφ and promoted the anti-inflammatory and pro-regenerative M2Mφ phenotype cells. Although pro-inflammatory M1Mφ cells progressively decreased, several M1Mφ cells were localized amongst oAECs. In addition, it was observed that some pro-inflammatory M1 CD86 positive cells co-localized with PKH26-oAECs suggesting an active in situ phagocytosis process. Differently, the

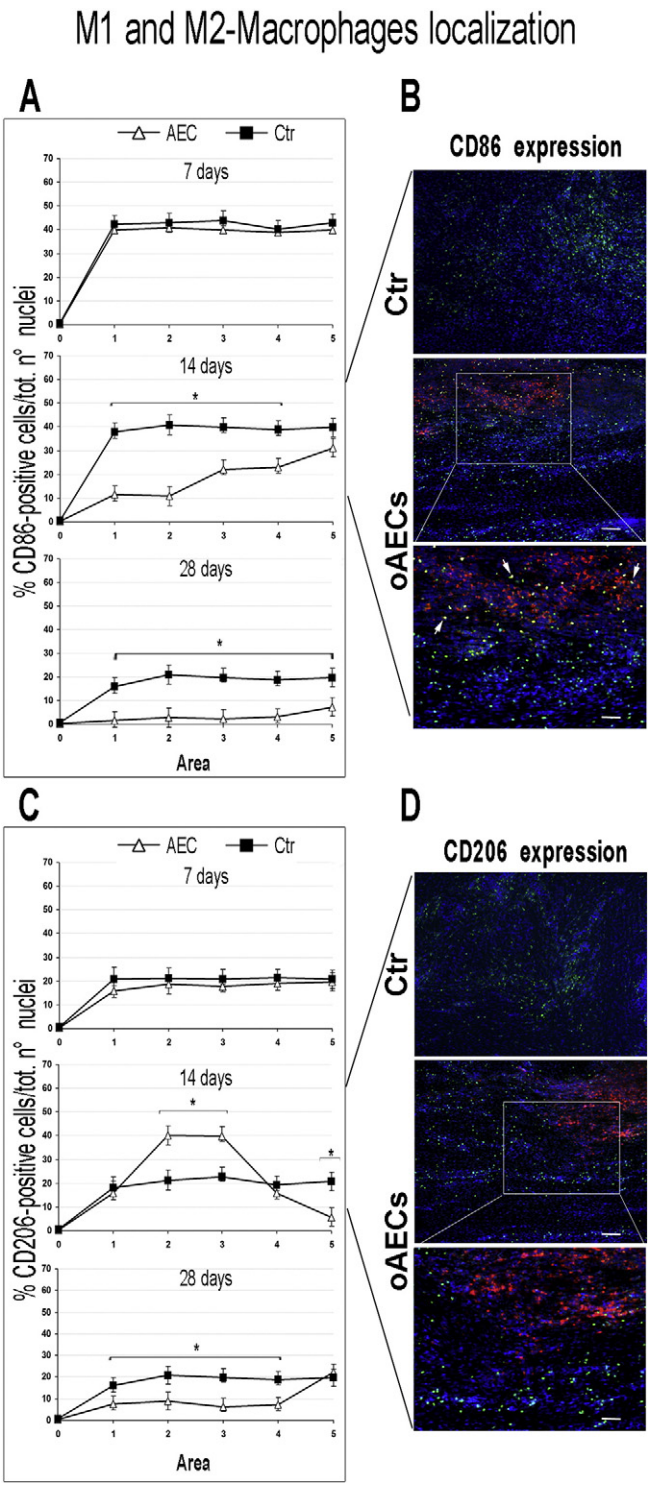

Fig. 6. Spatio-temporal modification of M1 and M2 macrophage subset populations. Quantification of (A) CD86 positive cell related to M1 macrophage and (C) CD206 positive cell related to M2 macrophage phenotypes in the defect area of healing tendons performed at 7, 14, and 28 days post treatment. The data of quantification are presented as median ± 25° and 75° percentile of 15 determinations/area/animal performed at 200× of magnification by capturing five images from six contiguous areas (indicated on x-axis as 0–5) starting from the healthy portion of the tissue (area 0) and proceeding throughout the repairing zone (1–3) to the core of the lesion (4–5). The side of each area analyzed was ~300 μm for an overall length of ~1800 μm. The final data considered for each time point are the median of 90 different determination (15 determination/area for 6 different animals/time point). *Significantly different values between Ctr and oAECs treated tendon. oAECs, tendon transplanted with amniotic epithelial cells; Ctr, contralateral tendon treated with only fibrin glue; M1 macrophage subset infiltration expressed as percentage of CD86 positive cells/total number of nuclei in the area; M2 macrophage subset infiltration, expressed as percentage of CD206 positive cells/total number of nuclei in the area. Representative images of (B) CD86 positive cell and (D) CD206 positive cells localization in Ctr (top image) and oAEC treated tendons at day 14 (central image). In the pictures PKH26-marked oAECs cells were visualized in red color whereas CD86 or CD206 positive cells were visualized in green color. Nuclei were counterstained with DAPI (blue color). Scale bar: 100 μm. In the inserts (B and D, bottom images), details of oAECs PKH26-marked cells (red color) and CD86 (green color) or CD206 positive cells (green color) localization in oAEC treated tendons, respectively. Arrows, indicated some CD86 (green color) and PKH26 positive (red color) cells co-localized giving a yellow merged fluorescence. Scale bar: 35 μm.

activation of the pro-regenerative M2Mφ phenotype population was not present in the whole repairing area, indeed this subset was spatially limited to the areas actively involved in extracellular matrix deposition and remodeling. This important Mφ spatial arrangement, and in particular of anti-inflammatory M2Mφ subset, was demonstrated by adopting sequential morphometric analyzes. This specific quantification allowed to describe oAECs centripetal repairing mechanism in situ that occurs in the host-injured tendons. The presence of M2Mφ was also confirmed by the analysis of the expression of their associated genes supporting the hypothesis that oAECs modulate M2 polarization at day 14, exactly when the allotransplanted tissue start to show a microarchitecture recovery. Indeed, the expression of M2 related cell surface marker CD206 as well as *YM1* and *IL10* genes showed a peak two weeks later oAECs transplantation. At day 28 oAECs treated tendons acquired a healthy-like structure, and contextually presented a reduction of M2Mφ phenotype cells and their markers, suggesting the ending of their pro-regenerative role. On the contrary, Ctr tissues maintained a high degree of disorganization and the pro-inflammatory M1Mφ markers persistency, hypothesizing an ongoing inflammation that probably yield to fibrotic scar formation. A rapid transition from the inflammatory to the reparative phase in oAECs allotransplanted tendons was also supported by the lower *IL12b* and *IL10* ratio indicating a Mφ skewing towards M2 phenotype, accordingly to Manuelpillai et al. (2012) observations in hAECs xeno-transplanted liver. This event appeared to be highly conserved since it accompanied also the fibrosis resolution of lung experimentally induced diseases (Manuelpillai et al., 2012; Abumaree et al., 2013; Moodley et al., 2013; Tan et al., 2014; Vosdoganes et al., 2013). The higher expression of *IL10* recorded at day 14 in oAEC treated tendons represents per se a positive repairing effect since this cytokine functions as a broad anti-inflammatory molecule able to prevent the production of IL1, TNF-α, IL12 and other pro-inflammatory factors (Fiorentino et al., 1991; D'Andrea et al., 1993; Hedrich and Bream, 2010; Li et al., 2014). The contemporary spatial distribution of M2Mφ phenotype in the areas of newly matrix deposition, strongly suggest that oAECs were able to orchestrate the complex tendon healing mechanisms. Indeed, according to Ariel and Timor (2013), Mφ and oAECs may have a balancing role on tissue repair and fibrosis by contributing both to the in situ release of TGFβ and VEGF (Barboni et al., 2012a), and of IL10, shown in this research. All these factors may also influence matrix degrading enzymes such as metalloproteinases MMPs and TIMPs inhibitors, all mediators involved in extracellular matrix remodeling (Mantovani et al., 2013). Even if the cause–effect relationship between oAECs and anti-inflammatory M2Mφ during tendon repair remains to be clarified, it could be hypothesized that a normal host macrophage function could be required for oAECs to exert their reparative effect. This assumption is supported by a recent work in which hAECs transplanted in surfactant deficient (Sftpc −/−) mice were unable to mitigate bleomicin induced lung injuries with impaired macrophage function (Murphy et al., 2012).

5. Conclusion

This study demonstrates that during the early phase of tendon regeneration induced by oAECs allotransplantation, Mφ infiltration represents a key event, mainly promoting pro-inflammatory M1Mφ towards anti-inflammatory and pro-regenerative M2Mφ phenotype skew. oAECs, probably through paracrine effects, reduce the presence of inflammatory CD45 and CD68 positive cells, and modulate M1Mφ and M2Mφ balance and distribution supporting tissue regeneration. The strict correlation between pro-regenerative M2Mφ distribution and microarchitecture recovery allows us to hypothesize an additional mechanism underlying oAECs mediated tendon healing. On the other hand, the results provide further evidence of oAECs immunomodulatory and anti-inflammatory effect supporting their pro-regenerative potential. Future studies should focus on the exact mechanisms by which Mφ polarization is modulated by oAECs, as well as oAECs potential to influence other key immune cell types and reparative pathways during tendon regeneration. In summary, these results give new insights into Mφ involvement during tendon regeneration after oAECs allotransplantation on a preclinical model. Overall, these results confirm potential for AEC-based regenerative therapies, and suggest cell-free alternative approaches that can respond to the clinical challenge related to animal and human tendinopathy therapies.

Author contributions

Conceived and designed the experiments: AMauro VR BB. Performed the surgical experiments: AMuttini. Performed the experiments: AMauro VR LDM. Analyzed the data: AMauro VR LDM PB AMartelli BB. Contributed reagents/materials/analysis tools: BB MM. Wrote the paper: BB AMauro VR. Critically revised paper: BB MM.

Conflict of interest

The authors have no conflict of interest to declare.

Acknowledgments

This work was supported by Tercas Foundation 2009 and by PRIN 2010–2011 (PRIN 20102ZLNJ5) financed by the Ministry of Education, University and Research (M.I.U.R.), Rome, Italy, BB is the author who received this funding. The funders had no role in study design, data collection and analysis, decision to publish, or preparation of the manuscript. We gratefully acknowledge the expert technical skills of O. Di Giacinto, D. Nardinocchi, D. Cocciolone and M. Turriani.

References

Abumaree, M.H., Al Jumah, M.A., Kalionis, B., Jawdat, D., Al Khaldi, A., Abomaray, F.M., Fatani, A.S., Chamley, L.W., Knawy, B.A., 2013. Human placental mesenchymal stem cells (pMSCs) play a role as immune suppressive cells by shifting macrophage differentiation from inflammatory M1 to anti-inflammatory M2 macrophages. Stem Cell Rev. 9 (5), 620–641.

Ariel, A., Timor, O., 2013. Hanging in the balance: endogenous anti-inflammatory mechanisms in tissue repair and fibrosis. J. Pathol. 229 (2), 250–263 (Review).

Ariel, A., Maridonneau-Parini, I., Rovere-Querini, P., Levine, J.S., Mühl, H., 2012. Macrophages in inflammation and its resolution. Front. Immunol. 3, 324. http://dx.doi.org/10.3389/fimmu.2012.00324.

Awad, H.A., Boivin, G.P., Dressler, M.R., Smith, F.N., Young, R.G., Butler, D.L., 2003. Repair of patellar tendon injuries using a cell–collagen composite. J. Orthop. Res. 21 (3), 420–431.

Banas, R.A., Trumpower, C., Bentlejewski, C., Marshall, V., Sing, G., Zeevi, A., 2008. Immunogenicity and immunomodulatory effects of amnion-derived multipotent progenitor cells. Hum. Immunol. 69 (6), 321–328.

Barboni, B., Russo, V., Curini, V., Mauro, A., Martelli, A., Mattini, A., et al., 2012a. Achilles tendon regeneration can be improved by amniotic epithelial cell allotransplantation. Cell Transplant. 21 (11), 2377–2395.

Barboni, B., Curini, V., Russo, V., Mauro, A., Di Giacinto, O., Marchisio, M., Alfonsi, M., Mattioli, M., 2012b. Indirect co-culture with tendons or tenocytes can program amniotic epithelial cells towards stepwise tenogenic differentiation. PLoS One 7 (2), e30974. http://dx.doi.org/10.1371/journal.pone.0030974.

Barboni, B., Mangano, C., Valbonetti, L., Marruchella, G., Berardinelli, P., et al., 2013. Synthetic bone substitute engineered with amniotic epithelial cells enhances bone regeneration after maxillary sinus augmentation. PLoS One 8 (5), e63256. http://dx.doi.org/10.1371/journal.pone.0063256 (17).

Barboni, B., Russo, V., Curini, V., Martelli, A., Berardinelli, P., Mauro, A., Mattioli, M., Marchisio, M., Bonassi Signoroni, P., Parolini, O., Colosimo, A., 2014. Gestational stage affects amniotic epithelial cells phenotype, methylation status, immunomodulatory and stemness properties. Stem Cell Rev. Rep. 10 (5), 725–741.

Bi, Y., Ehirchiou, D., Kilts, T.M., Inkson, C.A., Embree, M.C., Sonoyama, W., Li, L., Leet, A.I., Seo, B.M., et al., 2007. Identification of tendon stem/progenitor cells and the role of the extra-cellular matrix in their niche. Nat. Med. 13, 1219–1227.

Bowen, J.M., Chamley, L., Keelan, J.A., Mitchell, M.D., 2002. Cytokines of the placenta and extra-placental membranes: roles and regulation during human pregnancy and parturition. Placenta 23 (4), 257–273.

Brancato, S.K., Albina, J.E., 2011. Wound macrophages as key regulators of repair: origin, phenotype, and function. The American Journal of Pathology 178 (1), 19–25.

Bruns, J., Kampen, J., Kahrs, J., Plitz, W., 2000. Achilles tendon rupture: experimental results on spontaneous repair in a sheep-model. Knee Surg. Sports Traumatol. Arthrosc. 8 (6), 364–369.

Cargnoni, A., Gibelli, L., Tosini, A., Signoroni, P.B., Nassuato, C., Arienti, D., Lombardi, G., Albertini, A., Wengler, G.S., Parolini, O., 2009. Transplantation of allogeneic and

xenogeneic placenta-derived cells reduces bleomycin-induced lung fibrosis. Cell Transplant. 18 (4), 405–422.
Chen, J., Yu, Q., Wu, B., Lin, Z., Pavlos, N.J., Xu, J., Ouyang, H., Wang, A., Zheng, M.H., 2011. Autologous tenocyte therapy for experimental Achilles tendinopathy in a rabbit model. Tissue Eng. A 17 (15–16), 2037–2048.
Chong, A.K., Chang, J., Go, J.C., 2009. Mesenchymal stem cells and tendon healing. Front. Biosci. 14, 4598–4605.
Clarke, A.W., Alyas, F., Morris, T., Robertson, C.J., Bell, J., Connell, D.A., 2011. Skin-derived tenocyte-like cells for the treatment of patellar tendinopathy. The American Journal of Sports Medicine 39 (3), 614–623.
Colosimo, A., Curini, V., Russo, V., Mauro, A., Bernabò, N., Marchisio, M., et al., 2013. Characterization, GFP gene nucleofection, and allotransplantation in injured tendons of ovine amniotic fluid-derived stem cells. Cell Transplant. 22 (1), 99–117.
Dakin, S.G., Werling, D., Hibbert, A., Abayasekara, D.R., Young, N.J., Smith, R.K., Dudhia, J., 2012. Macrophage sub-populations and the lipoxin A4 receptor implicate active inflammation during equine tendon repair. PLoS One 7 (2), e32333. http://dx.doi.org/10.1371/journal.pone.0032333.
D'Andrea, A., Aste-Amezaga, M., Valiante, N.M., Ma, X., Kubin, M., Trinchieri, G., 1993. Interleukin 10 (IL-10) inhibits human lymphocyte interferon gamma-production by suppressing natural killer cell stimulatory factor/IL-12 synthesis in accessory cells. The Journal of Experimental Medicine 178 (3), 1041–1048.
Davies, L.C., Jenkins, S.J., Allen, J.E., Taylor, P.R., 2013. Tissue-resident macrophages. Nat. Immunol. 14 (10), 986–995.
Di Palma, S., Brunetti, B., Doherr, M.G., Forster, U., Hilbe, M., Zurbriggen, A., Vandevelde, M., Oevermann, A., 2012. Comparative spatiotemporal analysis of the intrathecal immune response in natural listeric rhombencephalitis of cattle and small ruminants. Comp. Immunol. Microbiol. Infect. Dis. 35 (5), 429–441.
Duerden, J.D., Keeling, J.J., 2008. Disorders of the Achilles tendon. Curr. Orthop. Prac. 19, 253–259.
Fiorentino, D.F., Zlotnik, A., Mosmann, T.R., Howard, M., O'Garra, A., 1991. IL-10 inhibits cytokine production by activated macrophages. J. Immunol. 147 (11), 3815–3822.
Gautier, E.L., Shay, T., Miller, J., Greter, M., Jakubzick, C., Ivanov, S., Helft, J., Chow, A., Elpek, K.G., Gordonov, S., Mazloom, A.R., Ma'ayan, A., Chua, W.J., Hansen, T.H., Turley, S.J., Merad, M., Randolph, G.J., 2012. Immunological genome consortium. Gene-expression profiles and transcriptional regulatory pathways that underlie the identity and diversity of mouse tissue macrophages. Nat. Immunol. 13 (11), 1118–1128.
Gordon, S., Martinez, F.O., 2010. Alternative activation of macrophages: mechanism and functions. Immunity 32 (5), 593–604.
Hedrich, C.M., Bream, J.H., 2010. Cell type-specific regulation of IL-10 expression in inflammation and disease. Immunol. Res. 47, 185–206.
Hoffmann, A., Pelled, G., Turgeman, G., Eberle, P., Zilberman, Y., Shinar, H., Keinan-Adamsky, K., Winkel, A., Shahab, S., Navon, G., Gross, G., Gazit, D., 2006. Neotendon formation induced by manipulation of the Smad8 signalling pathway in mesenchymal stem cells. J. Clin. Invest. 116 (4), 940–952.
Hou, Y., Mao, Z., Wei, X., Lin, L., Chen, L., Wang, H., Fu, X., Zhang, J., Yu, C., 2009a. Effects of transforming growth factor-beta1 and vascular endothelial growth factor 165 gene transfer on Achilles tendon healing. Matrix Biol. 28 (6), 324–335.
Hou, Y., Mao, Z., Wei, X., Lin, L., Chen, L., Wang, H., Fu, X., Zhang, J., Yu, C., 2009b. The roles of TGF-beta1 gene transfer on collagen formation during Achilles tendon healing. Biochem. Biophys. Res. Commun. 383 (2), 235–239.
Jarvinen, T.A., Kannus, P., Maffulli, N., Khan, K.M., 2005. Achilles tendon disorders: etiology and epidemiology. Foot and Ankle Clinics 10, 255–266.
Kuo, H.S., Tsai, M.J., Huang, M.C., Chiu, C.W., Tsai, C.Y., Lee, M.J., Huang, W.C., Lin, Y.L., Kuo, W.C., Cheng, H., 2011. Acid fibroblast growth factor and peripheral nerve grafts regulate Th2 cytokine expression, macrophage activation, polyamine synthesis, and neurotrophin expression in transected rat spinal cords. The Journal of Neuroscience 31 (11), 4137–4147.
Labonte, A.C., Tosello-Trampont, A.C., Hahn, Y.S., 2014. The role of macrophage polarization in infectious and inflammatory diseases. Mol. Cell 37 (4), 275–285.
Lange-Consiglio, A., Tassan, S., Corradetti, B., Meucci, A., Perego, R., Bizzaro, D., Cremonesi, F., 2013. Investigating the efficacy of amnion-derived compared with bone marrow-derived mesenchymal stromal cells in equine tendon and ligament injuries. Cytotherapy 15, 1011–1020.
Li, J., Koike-Soko, C., Sugimoto, J., Yoshida, T., Okabe, M., Nikaido, T., 2014. Human amnion-derived stem cells have immunosuppressive properties on NK cells and monocytes. Cell Transplant. ([Epub ahead of print] PubMed PMID:25333453).
Magatti, M., De Munari, S., Vertua, E., Nassauto, C., Albertini, A., Wengler, G.S., Parolini, O., 2009. Amniotic mesenchymal tissue cells inhibit dendritic cell differentiation of peripheral blood and amnion resident monocytes. Cell Transplant. 18 (8), 899–914.
Magatti, M., Caruso, M., De Munari, S., Vertua, E., De, D., Manuelpillai, U., Parolini, O., 2014. Human amniotic membrane-derived mesenchymal and epithelial cells exert different effects on monocyte-derived dendritic cell differentiation and function. Cell Transplant. http://dx.doi.org/10.3727/096368914X684033 [Epub ahead of print].
Malek, A., Bersinger, N.A., 2011. Human placental stem cells: biomedical potential and clinical relevance. Journal of Stem Cells 6 (2), 75–92.
Mamede, A.C., Carvalho, M.J., Abrantes, A.M., Laranjo, M., Maia, C.J., Botelho, M.F., 2012. Amniotic membrane: from structure and functions to clinical applications. Cell Tissue Res. 349 (2), 447–458.
Mantovani, A., Biswas, S.K., Galdiero, M.R., Sica, A., Locati, M., 2013. Macrophage plasticità and polarization in tissue repair and remodelling. J. Pathol. 229 (2), 176–185.
Manuelpillai, U., Lourensz, D., Vaghjiani, V., Tchongue, J., Lacey, D., Tee, J.Y., Murthi, P., Chan, J., Hodge, A., Sievert, W., 2012. Human amniotic epithelial cell transplantation induces markers of alternative macrophage activation and reduces established hepatic fibrosis. PLoS One 7 (6), e38631. http://dx.doi.org/10.1371/journal.pone.0038631.
Mattioli, M., Gloria, A., Turriani, M., Mauro, A., Curini, V., Russo, V., et al., 2012. Stemness characteristics and osteogenic potential of sheep amniotic epithelial cells. Cell Biol. Int. 36 (1), 7–19.
Mauro, A., Turriani, M., Ioannoni, A., Russo, V., Martelli, A., Di Giacinto, O., Nardinocchi, D., Berardinelli, P., 2010. Isolation, characterization, and in vitro differentiation of ovine amniotic stem cells. Vet. Res. Commun. 34 (Suppl. 1), S25–S28.
McCarty, R.C., Gronthos, S., Zannettino, A.C., Foster, B.K., Xian, C.J., 2009. Characterisation and developmental potential of ovine bone marrow derived mesenchymal stem cells. J. Cell. Physiol. 219 (2), 324–333.
Miki, T., 2011. Amnion-derived stem cells: in quest of clinical applications. Stem Cell Res. Ther. 2 (3), 25.
Moodley, Y., Ilancheran, S., Samuel, C., Vaghjiani, V., Atienza, D., Williams, E.D., Jenkin, G., Wallace, E., Trounson, A., Manuelpillai, U., 2010. Human amnion epithelial cell transplantation abrogates lung fibrosis and augments repair. Am. J. Respir. Crit. Care Med. 182 (5), 643–651.
Moodley, Y., Vaghjiani, V., Chan, J., Baltic, S., Ryan, M., Tchongue, J., Samuel, C.S., Murthi, P., Parolini, O., Manuelpillai, U., 2013. Anti-inflammatory effects of adult stem cells in sustained lung injury: a comparative study. PLoS One 8 (8), e69299. http://dx.doi.org/10.1371/journal.pone.0069299.
Mosser, D.M., Edwards, J.P., 2008. Exploring the full spectrum of macrophage activation. Nat. Rev. Immunol. 8 (12), 958–969.
Murphy, S.V., Atala, A., 2013. Amniotic fluid and placental membranes: unexpected sources of highly multipotent cells. Semin. Reprod. Med. 31 (1), 62–68.
Murphy, S., Lim, R., Dickinson, H., Acharya, R., Rosli, S., Jenkin, G., Wallace, E., 2011. Human amnion epithelial cells prevent bleomycin-induced lung injury and preserve lung function. Cell Transplant. 20 (6), 909–923.
Murphy, S.V., Shiyun, S.C., Tan, J.L., Chan, S., Jenkin, G., Wallace, E.M., Lim, R., 2012. Human amnion epithelial cells do not abrogate pulmonary fibrosis in mice with impaired macrophage function. Cell Transplant. 21 (7), 1477–1492.
Murray, P.J., Wynn, T.A., 2011. Protective and pathogenic functions of macrophage subsets. Nat. Rev. Immunol. 11 (11), 723–737.
Muttini, A., Mattioli, M., Petrizzi, L., Varavano, V., Sciarrini, C., Russo, V., Mauro, A., Cocciolone, D., Turriani, M., Barboni, B., 2010. Experimental study on allografts of amniotic epithelial cells in calcaneal tendon lesions of sheep. Vet. Res. Commun. 34 (Suppl. 1), S117–S120.
Muttini, A., Valbonetti, L., Abate, M., Colosimo, A., Curini, V., Mauro, A., et al., 2013. Ovine amniotic epithelial cells: in vitro characterization and transplantation into equine superficial digital flexor tendon spontaneous defects. Res. Vet. Sci. 94 (1), 158–169.
Neeland, M.R., Elhay, M.J., Nathanielsz, J., Meeusen, E.N., de Veer, M.J., 2014. Incorporation of CpG into a liposomal vaccine formulation increases the maturation of antigen-loaded dendritic cells and monocytes to improve local and systemic immunity. J. Immunol. 192 (8), 3666–3675.
Ni, M., Lui, P.P., Rui, Y.F., Lee, Y.W., Lee, Y.W., Tan, Q., et al., 2012. Tendon-derived stem cells (TDSCs) promote tendon repair in a rat patellar tendon window defect model. J. Orthop. Res. 30, 613–619.
Parolini, O., Alviano, F., Bagnara, G.P., Bilic, G., Bühring, H.J., Evangelista, M., Hennerbichler, S., Liu, B., et al., 2008. Concise review: isolation and characterization of cells from human term placenta: outcome of the first international workshop on placenta derived stem cells. Stem Cells 26 (2), 300–311.
Parolini, O., Soncini, M., Evangelista, M., Schmidt, D., 2009. Amniotic membrane and amniotic fluid-derived cells: potential tools for regenerative medicine? Regen. Med. 4 (2), 275–291.
Ruzzini, L., Abbruzzese, F., Rainer, A., Longo, U.G., Trombetta, M., Maffulli, N., Denaro, V., 2013. Characterization of age-related changes of tendon stem cells fsrom adult human tendons. Knee Surg. Sports Traumatol. Arthrosc. 22, 2856–2866.
Sharma, P., Maffulli, N., 2005. Tendon injury and tendinopathy: healing and repair. J. Bone Joint Surg. Am. 87, 187–202.
Sharma, P., Maffulli, N., 2006. Biology of tendon injury: healing, modeling and remodeling. J. Musculoskelet. Nueronal Interact. 6, 181–190.
Svensson, J., Jenmalm, M.C., Matussek, A., Geffers, R., Berg, G., Ernerudh, J., 2011. Macrophages at the fetal-maternal interface express markers of alternative activation and are induced by M-CSF and IL-10. J. Immunol. 187 (7), 3671–3682.
Tan, J.L., Chan, S.T., Wallace, E.M., Lim, R., 2014. Human amnion epithelial cells mediate lung repair by directly modulating macrophage recruitment and polarization. Cell Transplant. 23 (3), 319–328.
Vosdoganes, P., Wallace, E.M., Chan, S.T., Acharya, R., Moss, T.J., Lim, R., 2013. Human amnion epithelial cells repair established lung injury. Cell Transplant. 22 (8), 1337–1349.
Wagner, J.L., Storb, R., 1996. Preclinical large animal models for hematopoietic stem cell transplantation. Curr. Opin. Hematol. 3 (6), 410–415.
Wang, J.H., 2006. Mechanobiology of tendon. J. Biomech. 39 (9), 1563–1582.
Williams, T.J., Jones, C.A., Miles, E.A., Warner, J.O., Warner, J.A., 2000. Fetal and neonatal IL-13 production during pregnancy and at birth and subsequent development of atopic symptoms. J. Allergy Clin. Immunol. 105 (5), 951–959.
Wynn, T.A., Barron, L., 2010. Macrophages: master regulators of inflammation and fibrosis. Semin. Liver Dis. 30 (3), 245–257.
Young, M., 2012. Stem cell applications in tendon disorders: a clinical perspective. Stem Cells Int. 2012, 637836. http://dx.doi.org/10.1155/2012/637836.